A μSR study of magnetic ordering and metamagnetism in a bilayered molecular magnet

2007 J. Phys.: Condens. Matter 19 456208

(http://iopscience.iop.org/0953-8984/19/45/456208)

IOP PUBLISHING JOURNAL OF PHYSICS: CONDENSED MATTER

J. Phys.: Condens. Matter **19** (2007) 456208 (12pp) doi:10.1088/0953-8984/19/45/456208

A μSR study of magnetic ordering and metamagnetism in a bilayered molecular magnet

F L Pratt[1], P M Zieliński[2], M Bałanda[2], R Podgajny[3], T Wasiutyński[2] and B Sieklucka[3]

[1] ISIS Facility, Rutherford Appleton Laboratory, Chilton, Oxfordshire OX11 0QX, UK
[2] H Niewodniczański Institute of Nuclear Physics, Polish Academy of Sciences, Radzikowskiego 152, 31-342 Kraków, Poland
[3] Department of Chemistry, Jagiellonian University, Ingardena 3, 30-060 Kraków, Poland

Received 6 June 2007, in final form 17 August 2007
Published 11 October 2007
Online at stacks.iop.org/JPhysCM/19/456208

Abstract

Muon spin relaxation has been used to study the magnetic properties of a low-dimensional molecular magnet with a structure consisting of bilayers of $[W(CN)_8]^{3-}$ and Cu^{2+}. In the magnetically ordered state a spontaneous precession signal was found to contain two main components and the temperature dependence of the characteristic internal fields was followed up to the critical temperature. The critical exponent obtained for the magnetic order parameter $\beta = 0.237(12)$ points to the two-dimensional character of the transition and reflects its underlying Berezinski–Kosterlitz–Thouless nature. Experiments performed in the longitudinal magnetic field demonstrate clearly a spin-flip phenomenon associated with the weak inter-bilayer coupling, that takes place in the magnetic field region below 100 G. The muon precession signals measured in the vicinity of this transition provide detailed local information about the corresponding rearrangements of the spin structure.

1. Introduction

One of the reasons for considerable interest in molecular magnetism is the possibility to engineer structures of low dimensionality, i.e. zero-dimensional (0D) molecular clusters, one-dimensional (1D) chains or two-dimensional (2D) layered networks. Novel magnetic behaviour observed in such systems with reduced dimensionality makes them attractive both for fundamental research and for possible applications. Quite often, real molecular magnets are not ideal model systems, but are actually situated somewhere between 1D and 2D or 3D, or between 2D and 3D, in such a way that the 3D magnetic ordering appears at low temperatures, often due to the dipolar interaction between low-dimensional correlated spin clusters. An effective method to study magnetic molecular materials is the μSR technique, which uses muons as a local magnetic probe that can follow the temperature dependence

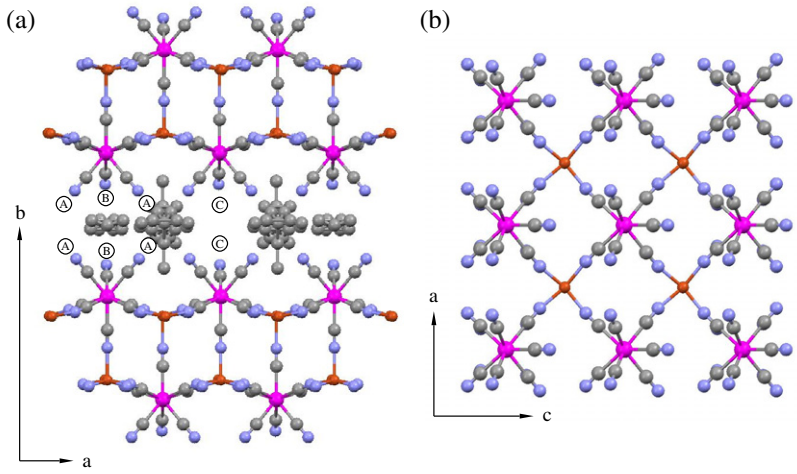

Figure 1. Illustration of the crystal structure of WCuT projected onto the *ab* plane (a) and one half of the bilayer projected onto the *ac* plane (b). The muon sites discussed in the text (A, B and C) are marked in (a). Sites C are are symmetrically placed about one of the tetren vacancies, which is placed the centre of (a).

(This figure is in colour only in the electronic version)

of order parameters, as well as providing information about local internal fields, magnetic fluctuations and spin dynamics [1, 2].

In this paper we present the results of μSR measurements performed on the copper octacyano-tungsten compound $(\text{tetrenH}_5)_{0.8}\text{Cu}^{\text{II}}_4[\text{W}^{\text{V}}(\text{CN})_8]_4{\cdot}7.2\text{H}_2\text{O}$ (hereafter abbreviated as WCuT). This compound has a unique bilayered structure [3] (figure 1) constructed from anionic double layers of $\text{Cu}^{\text{II}}[\text{W}^{\text{V}}(\text{CN})_8]^-$ aligned in the *ac* plane. The space between these bilayers is filled with water molecules and fully protonated tetren molecules (tetren = tetraethylenepentaamine). The occupancy of the tetren sites is 80%, implying that one in five of these sites is vacant. Every Cu ion is coordinated by five CN groups bridged to a W ion, while each W ion has five CN bridges to Cu ions and three others remaining unbridged. Figure 1 shows the crystal structure projected onto the *ab* plane and one of the Cu–W layers projected onto the *ac* plane.

Investigations of the magnetic properties of this compound, carried out for powder [3–5] and single crystal [6] samples, have revealed the interesting quasi-2D properties of this system. In the paramagnetic region the magnetic correlations between the Cu^{II} ($S = 1/2$) and W^{V} ($S = 1/2$) ions are of the ferromagnetic (FM) type with a positive Curie–Weiss temperature $\Theta \approx 50$ K. The transition to the magnetically ordered state was observed at $T_{\text{c}} = 33.4$ K. It follows from the single crystal study [6] that the compound is strongly anisotropic, with magnetic moments lying in the *ac* plane (easy plane). There is a small XY anisotropy present in the bilayers. A weak antiferromagnetic (AF) coupling between the double layers comes from their dipolar interaction. An applied magnetic field $B = \mu_0 H \approx 100$ G (at 4.2 K) parallel to the easy plane brings about a spin-flip, which drives the system from the AF state into a fully FM ordered state. In the μSR experiment reported here it was possible to determine the temperature dependence of the internal magnetic fields, which directly scale with the magnetic order parameter. It was also possible to observe directly the behaviour of the internal field at two distinct muon sites as the sample undergoes the spin-flip transition.

2. Experimental details

The experiment was carried out at the ISIS pulsed muon facility using the MuSR instrument. The polycrystalline powder sample was mounted in one of two cryostats used for the measurement, the first cryostat was a closed cycle refrigerator providing temperatures down to 11 K and the second cryostat employed a helium bath to give temperatures down to 1.8 K. The time evolution of the spin polarization $P(t)$ of the implanted muons was detected by measuring the asymmetry $A(t)$ of the number of emitted forward N_{F} and backward N_{B} decay positrons as a function of time, defined as

$$A(t) = \frac{N_{\mathrm{B}} - N_{\mathrm{F}}}{N_{\mathrm{B}} + N_{\mathrm{F}}}. \tag{1}$$

The temperature scans were performed for zero external field (ZF) and for a small longitudinal external fields of 20–30 G (LF). The precision of the temperature measurement associated with a run was generally better than 10 mK, although it is estimated that the absolute accuracy of the temperature is no better than 0.1 K, due to calibration errors and thermal offset between sample and thermometer. The size of the critical region around a magnetic transition in reduced temperature units $t = |T - T_{\mathrm{c}}|/T_{\mathrm{c}}$ is determined by the Ginzburg number G, which is dependent on the effective dimensionality d and the effective interaction range R, following the form $G \propto R^{-2d/(4-d)}$ [7]. The short range interactions in a local moment AF naturally lead to a relatively broad critical region and working with a low-dimensional layered system can broaden the critical region still further, since $G_{2\mathrm{D}} = G_{3\mathrm{D}}^{1/3}$ for a given R. For example, if a 3D system has a fairly narrow $G_{3\mathrm{D}} \sim 0.05$, the corresponding 2D system with the same R would be expected to have a much broader $G_{2\mathrm{D}} \sim 0.4$. As a result of the large size of the 2D critical region in the present system, temperature measurement is not a major limitation in extracting the 2D critical properties, whereas the much narrower 3D region provides a greater experimental challenge.

In order to study with muons the spin-flip transition that occurs under an applied magnetic field, a constant temperature field scan was made at 14 K with the applied longitudinal field being varied in steps between 0 and 200 G.

3. Results

3.1. Muon spin rotation

The transition to the ordered magnetic state upon cooling from the paramagnetic phase is clearly seen from the onset of spontaneous oscillations in the zero field relaxation signal below 33 K (figure 2), demonstrating the presence of local fields which are static on the microsecond timescale. The oscillatory part of the asymmetry is well described by the sum of two frequency components ω_1 and ω_2

$$A(t) = A_1 \cos(\omega_1 t)\mathrm{e}^{-\lambda_1 t} + A_2 \cos(\omega_2 t)\mathrm{e}^{-\lambda_2 t}, \tag{2}$$

where $\omega_i = \gamma_\mu B_i$, $\gamma_\mu = 2\pi \times 1.355 \times 10^8$ s^{-1} T^{-1}, B_i is the size of the magnetic field at each muon site and λ_i is the relaxation rate. The amplitude of the lower frequency component was found to be about twice that of the higher frequency component. The damping of the oscillations is such that they are confined to times below 5 μs and thus the fits of the precession signals were performed over the range 0–5 μs.

The temperature dependence of the two local magnetic fields, B_1 and B_2, corresponding to the two precession signals is shown in figure 3. Both components can be fitted to the phenomenological function [8]

$$B_i(T) = B_i(0)[1 - (T/T_{\mathrm{c}})^{\alpha}]^{\beta}. \tag{3}$$

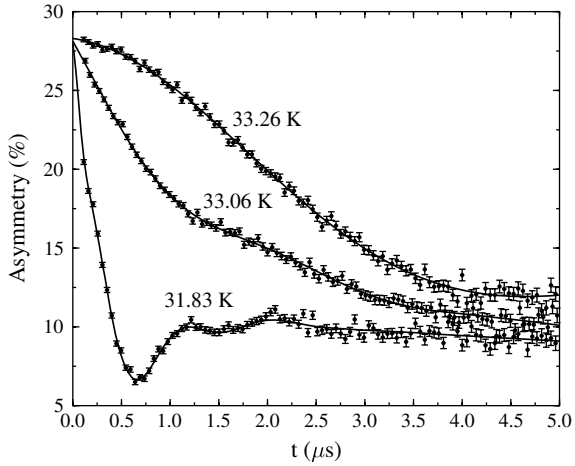

Figure 2. Temperature dependence of the zero field muon spin relaxation in the vicinity of the magnetic transition.

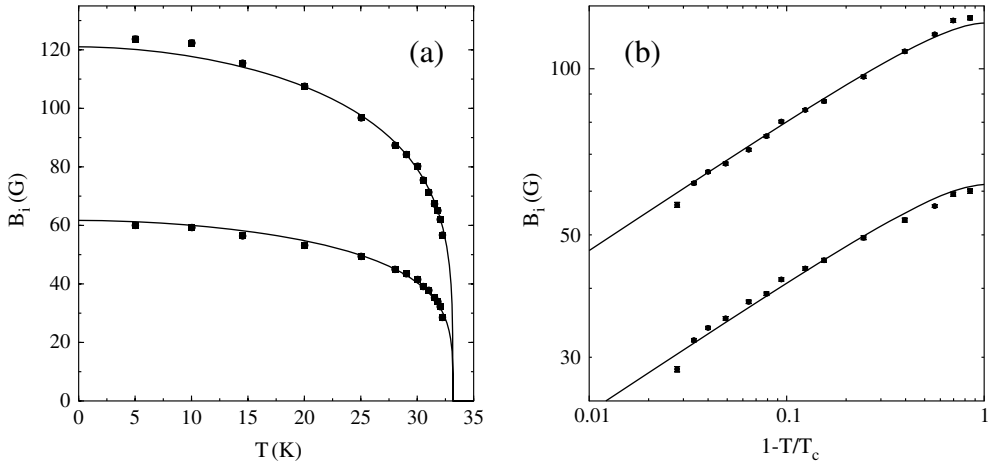

Figure 3. Temperature dependence of the local fields B_1 and B_2 in (a) linear and (b) scaling plot form with solid lines showing the fits to (3).

The α parameter in (3) allows for a low T behaviour governed by spin-wave excitations, whereas β determines the asymptotic critical behaviour close to the transition. The onset of the magnetic precession signal lies somewhere between 33.06 and 33.26 K on the scale of our thermometer (see figure 2) and we therefore take the midpoint of these limits, 33.16 K, as the best estimate of T_c, with an associated uncertainty of ± 0.1 K. Taking this value for T_c, the other parameters in (3) were determined simultaneously from fitting both sets of local fields over the full temperature range 5–33 K, giving $\beta = 0.237(12)$, $\alpha = 1.84(15)$ and $B_i(0)$ values 121.0(6) G and 61.7(7) G for component 1 and component 2 respectively (figure 3). The measured critical exponent β is consistent with the effective value of 0.231 expected for a 2D XY system [9] and the relatively wide critical region is again consistent with expectations for a 2D local moment system. To search for possible crossover behaviour close to T_c, fits were made as a function of T_{min}, the lower bound of the fitting range, fixing α to the value obtained from the full range fit. The results are shown in figure 4, from which it can be seen that β remains close to the 2D XY value until the reduced temperature range falls below 0.2 where it starts

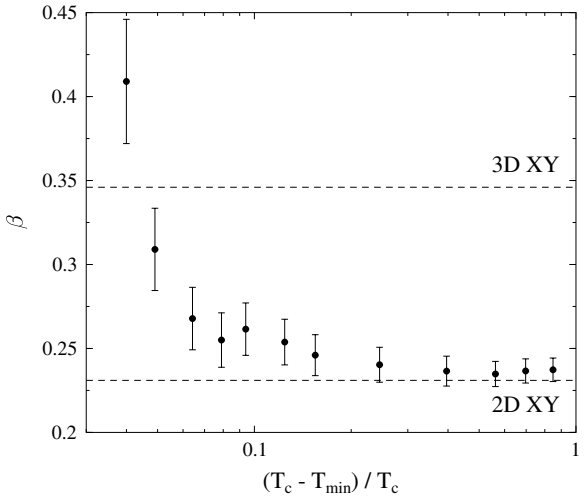

Figure 4. Dependence of the fitted value for β on the temperature range used for the fit. Dashed lines indicate the theoretical values expected for the 3D XY and 2D XY models. A crossover from 2D XY to 3D XY behaviour is suggested when the fit is restricted to the region very close to the transition.

to increase towards the 3D XY value of 0.349 [10], suggesting a dimensional crossover. Data within the reduced temperature range 0.05 are reasonably consistent with the 3D XY value, given the increased uncertainty of these points due to the reduced number of data points in the fit.

In order to compare the proposed magnetic structure with the experimentally measured local field values, the dipolar field distribution $\mathbf{B}(\mathbf{r})$ produced within the crystal structure by the ordered atomic moments was obtained by summing the contributions from the atomic moments $\mathbf{m}_i$ at lattice positions $\mathbf{d}_i$,

$$\mathbf{B}(\mathbf{r}) = \sum_i \frac{\mu_0}{4\pi r_i^3}\left(\mathbf{m}_i - \frac{3}{r_i^2}(\mathbf{m}_i \cdot \mathbf{r}_i)\mathbf{r}_i\right), \qquad \mathbf{r}_i = \mathbf{r} - \mathbf{d}_i. \tag{4}$$

The sum is evaluated for the spins within a Lorentz sphere of radius r_L which is large enough to ensure convergence and to get the total field an additional Lorentz contribution $\mathbf{B}_\mathrm{L}$ from spins outside the Lorentz sphere must be added, which is zero for the AF case and directly proportional to the domain magnetization in the FM case. For the calculations it was assumed that the Cu and W each have moment 1 μ_B and the couplings within the bilayer are all FM with easy axis within the layers and the inter-bilayer coupling is either AF or FM. The resulting field maps were surveyed carefully over the magnetic cell. The presence of two well-defined muon precession frequencies suggests either two distinct muon sites within the structure or alternatively a single site where the internal field depends on the spin alignment of the local domain. The expected stopping sites for positive muons are close to negatively charged regions in the structure, such as the CN groups or the cavities associated with the 20% of cation sites that are vacant. In the WCuT structure (figure 1) five of the CN groups around a W form links to Cu ions, one in axial orientation provides the link between the two halves of the bilayer and the other four in approximate equatorial configuration provide the links within the layers. The remaining three CN groups, directed outwards from the bilayer, remain unbridged and so might be considered to provide attractive stopping sites for a muon. Two out of these three CN groups are symmetry equivalent by reflection in the bc plane, thus if we assume muon

Table 1. Local fields at three possible muon sites (see figure 1) for different orientations within the ac plane for the axis of the ordered moments. Sites A and B are coordinated to unbridged CN groups, whereas site C lies at a higher symmetry position near a tetren vacancy. Site C is displaced from the centre of this vacancy towards the three unbridged CN groups of the nearest W atom, which is at (0 0.145 0). Field magnitudes are shown for the case of AF and FM coupling between adjacent bilayers. The final two columns list the angle θ that the field makes to the spin axis in each case.

Site	Spin axis	B_{AF} (G)	B_{FM} (G)	$B_{\mathrm{FM}} - B_{\mathrm{AF}}$ (G)	θ_{AF} (deg)	θ_{FM} (deg)
A	a	102.7	102.3	−0.4	46	40
(0.377 0.043 −0.154)	c	36.2	36.4	0.2	67	73
	$a + c$	57.8	52.7	−5.1	91	83
	$a - c$	92.2	94.9	2.7	49	47
B	a	28.6	41.2	12.6	0	0
(0.000 0.059 0.496)	c	191.5	178.6	−12.9	2	3
	$a + c$	136.9	129.6	−7.0	55	59
	$a - c$	136.9	129.6	−7.0	55	59
C	a	62.5	82.1	19.6	180	180
(0.000 0.036 0.000)	c	116.9	138.7	21.8	82	83
	$a + c$	93.7	113.9	20.2	105	107
	$a - c$	93.7	113.9	20.2	105	107

sites associated evenly with these groups, a 2:1 ratio corresponding to the measured amplitude ratio of the precession components would follow naturally. A likely configuration for a muon associated with one of these unbridged CN groups would follow the linear geometry of HCN, i.e. C–N–μ with the N–μ distance being 0.1 nm (sites A and B). Another location that would be an attractive site for a positive muon would lie in the negatively charged tetren cavity: within this cavity the local field varies smoothly with the distance away from the bilayer containing the magnetic moments. It is found that a site displaced slightly away (by 0.11 nm) from the centre of the cavity along the b axis towards one of the bilayers and the mean position of the unbridged trio of CN (site C) has a local field consistent with B_1 for spins aligned with the c axis and a field consistent with B_2 for a axis spin alignment.

The local fields obtained at the A, B and C sites discussed here are listed in table 1 where the effects of different spin orientations within the layer plane and of changing the mode of interlayer coupling are explored. From table 1 it is seen that the scale of fields obtained for these example sites matches well with those observed from experiment, confirming that it is a reasonable assumption that the muon sites lie in the region between the bilayers. For comparison, regions of the crystal lattice around the intralayer and layer-bridging CN groups all have much higher local fields, ranging from just over 200 G to more than 2000 G.

3.2. Muon spin relaxation

The relaxation rate of the muon polarization was determined from the long time behaviour of the asymmetry $A(t)$ in the time range after the oscillatory behaviour has been strongly damped away (3–32 μs). Fitting was made to the relaxation functions:

$$A(t) = a_{\mathrm{rel}} \mathrm{e}^{-\lambda t} \qquad T < T_{\mathrm{c}} \tag{5}$$

$$A(t) = a_{\mathrm{rel}} \mathrm{e}^{-\lambda t} G^{\mathrm{KT}}(\Delta, B, t) \qquad T > T_{\mathrm{c}}, \tag{6}$$

where G^{KT} is the static Kubo–Toyabe function [11] describing the nuclear dipolar contribution to the relaxation. The phase transition manifests itself as a sharp fall in the relaxing asymmetry

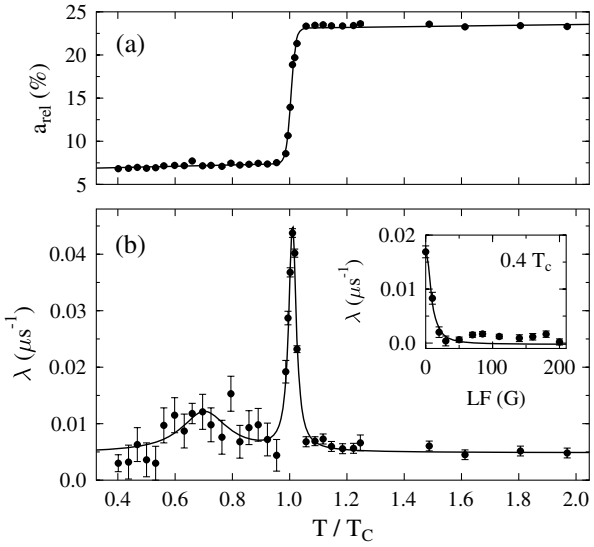

Figure 5. (a) Temperature dependence of the non-oscillatory asymmetry measured in a 20 G longitudinal field and (b) the corresponding relaxation rate λ. The solid line in (b) is a fit to two Lorentzians. The inset shows λ as a function of longitudinal field for a temperature of 14 K ($0.4T_c$), fitted to (8).

a_{rel} (figure 5(a)) and as a sharp peak in the relaxation rate (figure 5(b)). Within the ordered state below the transition there is also a second broad and weak relaxation peak. This relaxation below T_c is strongly suppressed by applied field and detailed measurements at fields in the range 0–200 G for a constant temperature of 14 K are shown in the inset to figure 5(b). The muon relaxation can be described here in terms of the relaxation of the field–field correlation function as follows [12]

$$\lambda = \int_0^\infty \gamma_\mu^2 \langle B_\perp(t) B_\perp(0) \rangle \cos \gamma_\mu B_L t \, dt, \tag{7}$$

where B_L is the longitudinal field. Assuming $\langle B_\perp(t) B_\perp(0) \rangle = \langle B_\perp^2 \rangle e^{-t/\tau}$ and $\langle B_\perp^2 \rangle = 2(\Delta_f/\gamma_\mu)^2$, where τ is the field–field correlation time, the following Lorentzian field dependence is obtained for λ:

$$\lambda = \frac{2\Delta_f^2 \tau}{1 + (\gamma_\mu B_L \tau)^2}. \tag{8}$$

The solid line in the inset to figure 5(b) represents a fit to (8) with parameters $\Delta_f = 0.073(5)\ \mu s^{-1}$ and $\tau = 1.5(2)\ \mu s$. The corresponding root-mean-square field at the muon site is $\sqrt{2}(\Delta_f/\gamma_\mu) = 1.2(1)$ G. The field amplitude associated with the fluctuation is thus 50–100 times smaller than the static field values at the muon sites obtained from the spin rotation. One interpretation of the small amplitude field fluctuation is that it reflects the dipolar field contribution from the next-nearest bilayer to the muon site and 1.2 G would be broadly consistent with the calculated range of B_{FM}–B_{AF} for site A, whereas a larger field amplitude would be expected for sites B and C (table 1). In view of the dominant 2D character of the main transition at 33 K, the slow fluctuations seen below 30 K can be viewed as a reflection of the weak interlayer coupling which allows thermal fluctuations to easily perturb the fragile 3D interlayer order.

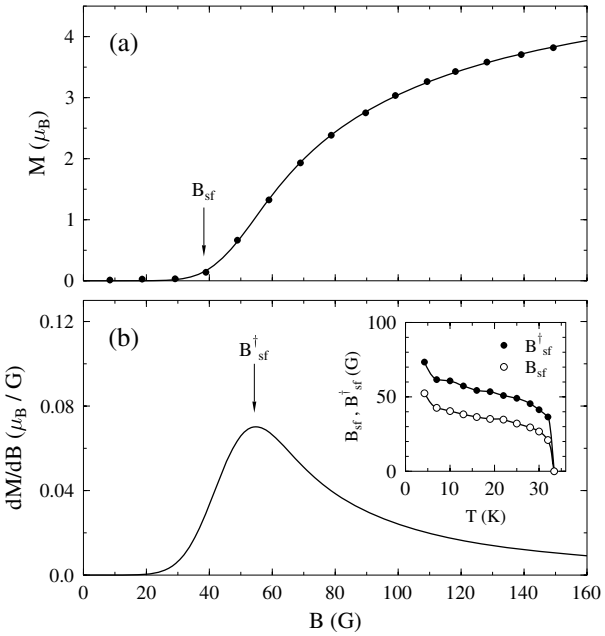

Figure 6. Magnetization curve (a) and its derivative (b) for WCuT at 14 K with arrows showing schematically the start point B_{sf} and the inflection point $B^{\dagger}_{sf}$ for the transition. The inset shows the temperature dependence of these fields.

3.3. Spin-flip transition

As mentioned earlier, the system under study shows metamagnetic behaviour and a relatively weak magnetic field applied parallel to the *ac* plane induces a spin-flip in which the mode of ordering between successive bilayers is believed to switch over from AF to FM. For a powder sample, the magnetization change at the transition becomes broadened, as it is averaged over the distribution of randomly oriented grains. Figure 6 shows the 14 K magnetization curve and its derivative for WCuT with arrows on the curves showing schematically the start point and inflection point for the transition. The temperature dependence of the relevant fields is given in the inset.

In order to use muons to provide a local probe of this spin reorientation process, a field scan with the applied longitudinal field changed from 0 up to 200 G was performed at constant temperature of 14 K. The expected change of the muon spin rotation frequency and amplitude under applied longitudinal field in the static case, i.e. when magnetic structure is not perturbed, is considered in an accompanying paper [13]. There is no significant effect expected for applied fields smaller than the characteristic internal field in the ordered phase. For applied fields significantly higher than the original internal field, a linear increase of the muon spin rotation frequency should be observed. In the case when the applied field modifies the spin arrangement, deviation of the field-dependent muon polarization parameters from the behaviour expected for a fixed spin structure will result. Results of the total precession amplitude for the LF scan performed at 14 K are presented in figure 7(a). The theoretical behaviour expected for a fixed magnetic structure is shown with a solid line; this is entirely defined by the precession amplitudes and fields observed in the zero field measurement, following a well-defined set of analytical equations [13]. The main features of deviation of the sum from the static case (figure 7(b)) are seen to map reasonably well onto the powder magnetization data (figure 6(a)). In this plot a fully static region is seen up to $B_{st} \sim 15$ G. Above this point the asymmetry decreases steadily with field, probably reflecting a spin reorientation process within the easy plane in response to the in-plane component of the applied field $B_{\parallel}$, e.g. a spin–flop phase where

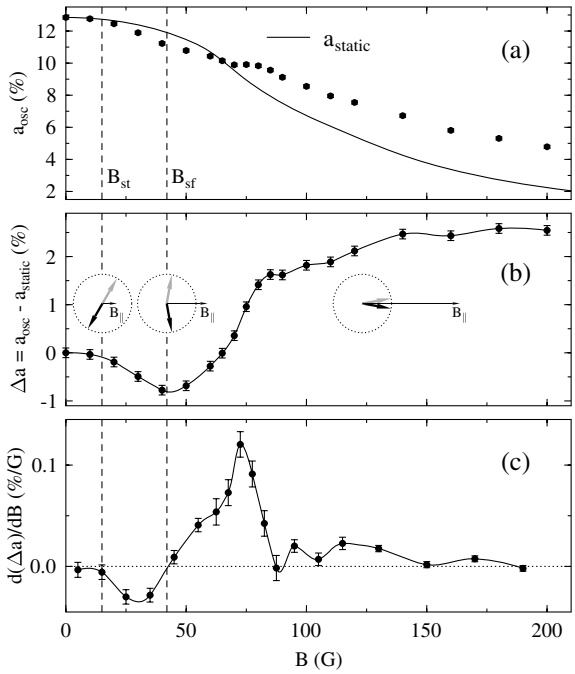

Figure 7. (a) Sum of the precession amplitudes for the two signals as a function of LF for $T = 14$ K, along with the prediction for the spin distribution remaining fixed at its zero field configuration. (b) shows the deviation Δa of the measured amplitude from the static dependence. $B_{\rm st}$ is the threshold field for deviation from static behaviour and $B_{\rm sf}$ is the threshold field for the onset of the spin-flip transition. Dependence of the orientation of the two AF sublattices on the in-plane component of applied field $B_\parallel$ is illustrated for a typical crystallite. (c) shows the derivative of Δa with respect to B, which can be compared with the bulk magnetization derivative of figure 6(b).

the spin axis initially rotates to being close to 90° to $B_\parallel$. At $B_{\rm sf} \sim 40$ G this behaviour changes, reflecting the onset of the spin-flip transition in which the bilayers become fully FM aligned with each other. The midpoint of the main spin-flip transition is around 70 G and saturation of the deviation occurs around 140 G. This is generally consistent with what has been obtained from the bulk magnetic measurements and demonstrates the good sensitivity of the muons to the details of the spin rearrangement.

Comparing more closely the bulk magnetic response of figure 6 and the local probe signal of figure 7 it is clear that some additional structure is seen in the muon data, suggesting that the muon is seeing some local changes taking place in the spin structure that do not affect the bulk magnetization. More detailed information may be gained about these local changes by looking at the field dependence of the two muon precession signals individually. The dependence of the two precession signals is plotted in figure 8 along with the behaviour for each signal predicted by its zero field parameters. Although the main deviation in precession frequency and amplitude from the static case takes place around 70 G for both signals, corresponding to the peak in figure 7(c), some differences in behaviour are apparent. In particular the B_1 signal starts to deviate from static behaviour near the bulk spin-flip threshold of 40 G, whereas the B_2 signal follows its static curve until 70 G. When the spin transitions are essentially complete above 140 G the B_2 signal returns again to the static value, whereas the B_1 signal in the high field region shows a large constant negative deviation from the static line, which is of the order of 60 G. These results indicate that significant changes in the magnitude and

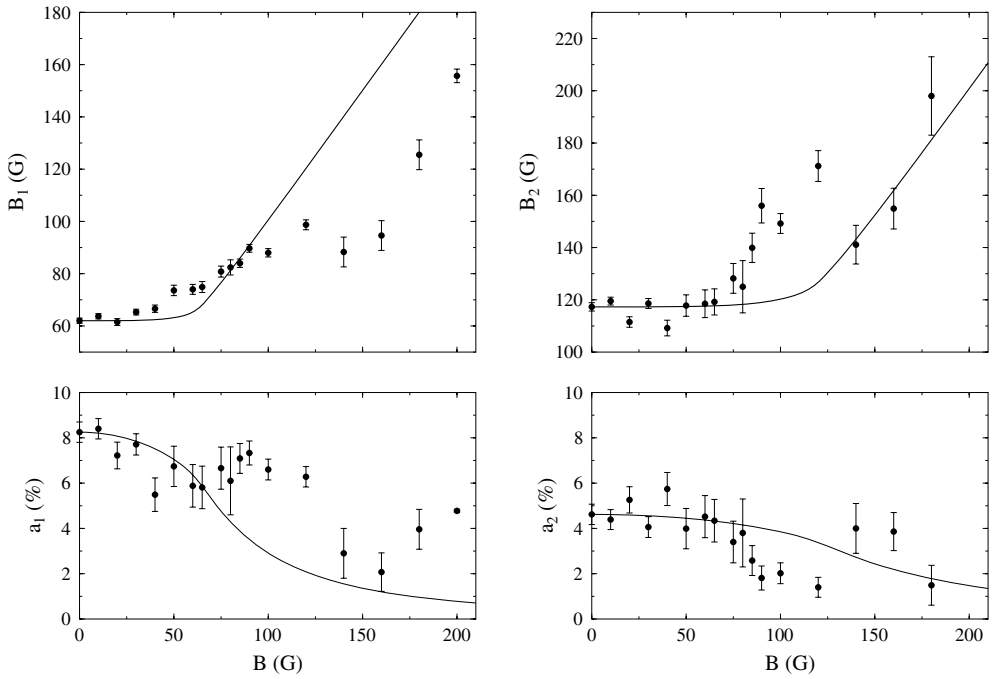

Figure 8. LF dependence of the two precession components at 14 K. The upper plots show the precession field and the lower plots the precession amplitude. Solid lines show the behaviour expected in each case for a static spin distribution that is independent of field.

direction of the local field are taking place at the muon sites. In order to understand the origin of some of the features in figure 8 it is useful to look at the expected behaviour for different orientations of the local field in relation to the applied field direction. Figure 9 illustrates this behaviour for a local field of magnitude $B_0 = 50$ G. The deviation of a precession field B_i from the applied field $B_{\rm app}$ in the high field region follows $B_0 \cos\theta$ and may therefore be positive or negative. Negative deviation corresponds to $\theta > 90°$ and in this case a peak in the precession amplitude a_i is expected at or below B_0. When $\theta < 90°$ the deviation is positive and the amplitude is suppressed compared to the case of random orientation. In the high field region where the spin-flip transition is complete the spins will be oriented parallel to the in-plane component of the applied field, so the θ value will determine the type of behaviour seen, although orientational averaging might be expected to give some smoothing out of the characteristic behaviour. Referring back to figure 8 it can be seen that B_1 does indeed show features associated with $\theta > 90°$ (i.e. negative $B_i - B_{\rm app}$ and a peak in a_i), whereas B_2 shows features associated with $\theta < 90°$ (positive $B_i - B_{\rm app}$ and a suppression of a_i). From table 1 it can be seen that only site C is able to produce the range of θ values needed to describe both the magnitude and direction of the fields defining the precession signals. As noted earlier, for site C the field B_1 is obtained for spin axis $s \parallel a$ and B_2 is obtained for $s \parallel c$. Since these field values are extrema of the orientational distribution, they will dominate the angular average and thus the observed muon precession signal. We therefore conclude that all of the muon precession data can be described by the single muon site C, with the ordered spin structure taking a range of orientations within the XY symmetry plane. Since the B_1 signal has larger amplitude than B_2, this suggests that weak anisotropy within the XY plane may be marginally favouring domains with a axis orientation for the spins.

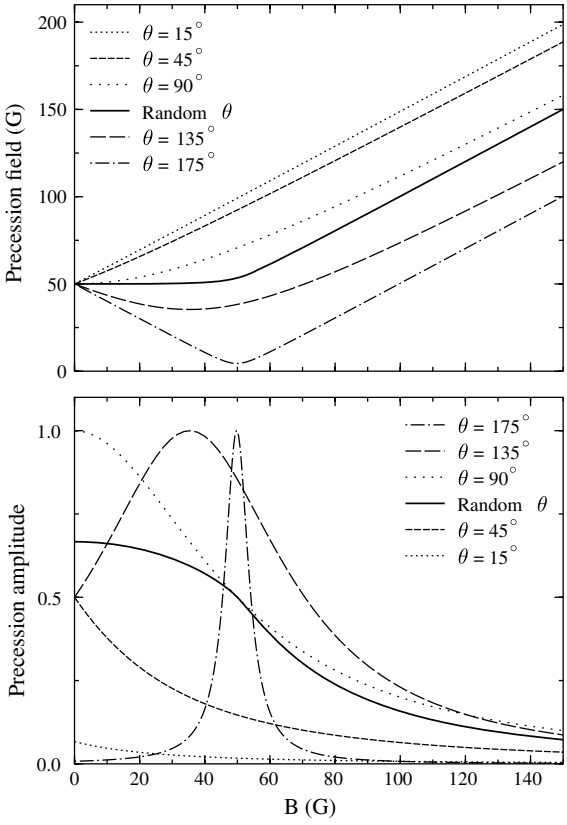

Figure 9. Expected LF dependence of the precession field and amplitude for a local field of 50 G at different fixed orientations with respect to the applied field, compared with the random orientationally averaged behaviour [13].

4. Discussion and conclusion

The muon spin rotation and relaxation measurements reported here have shed some new light on the magnetic ordering and the nature of the field-induced phase transformation for this unusual bilayered molecular magnet system. Based on the analysis of the dipolar local field distributions for various models of the ordered magnetic structure, it was concluded that a muon stopping site associated with a tetren vacancy is most likely, being consistent with both the XY anisotropy of the magnetic ordering and with the behaviour of the muon signals on traversing the field-induced metamagnetic transition. Both fields characterizing the precession signal, which are a measure of the magnetic order parameter, follow the power law scaling form of (3) over a wide range of temperature. The value of the critical exponent β and the extended width of the critical region support the 2D XY character of WCuT. A similarly wide range of critical behaviour has been recently observed for the quasi-2D antiferromagnet $MnPS_3$ [14] and a recent μSR study of the critical properties of the layered antiferromagnet cobalt glycerolate [15] also found a wide critical region with a β value of 0.23, however that system has a highly non-collinear spin structure and the critical behaviour was found to conform to a 3D non-collinear XY model. There is no evidence for any non-collinearity in the spin structure of the present system however and the combination of the β value derived here alongside specific features of the field cooled magnetization and susceptibility [6] and specific heat [16], all suggest that the phase transition at T_c is essentially of the Berezinski–Kosterlitz–Thouless type [17], where the thermal excitation of magnetic vortices in the 2D layers is a

dominant feature and the magnetic correlation length ξ on approaching the transition from above follows the specific BKT exponential divergence $\xi \sim \exp(bt^{-1/2})$ with $b \sim 1.5$ over an extended range of temperature [17, 6], in contrast to the power law divergence of standard critical scaling theory.

In this study the μSR technique has proved to be very successful in directly monitoring the field-induced spin reorientation process and has suggested some additional complexity in the transition that was not apparent from simply observing the bulk magnetization. The results highlight the potential of μSR in the study of metamagnets. In this context another muon study of a molecular magnet showing a metamagnetic transition, ferrocene–TCNQ, was reported recently [18]. Spontaneous precession could not however be observed in that measurement and the metamagnetic transition was revealed through an increase in the overall broadening of the muon spin rotation signal when the transverse applied field exceeded 0.13 T, which was assigned to the appearance of demagnetizing fields in the field-induced ferromagnetic state. As far as we are aware, the results presented in the current study represent the first observation of a metamagnetic transition using well-resolved muon precession signals as site-specific local probes.

Acknowledgment

This research project has been supported by the European Commission under 6th Framework Programme through the Key Action: Strengthening the European Research Area, Research Infrastructures. Contract no. RII3-CT-2003-505925.

References

[1] Blundell S J 2001 *Magnetism: Molecules to Materials* ed J S Miller and M Drillon (New York: Wiley–VCH) p 235
[2] Blundell S J and Pratt F L 2004 *J. Phys.: Condens. Matter* **16** R771
[3] Podgajny R, Korzeniak T, Bałanda M, Wasiutyński T, Errington W, Kemp T J, Alcock N W and Sieklucka B 2002 *Chem. Commun.* 1138
[4] Sieklucka B, Korzeniak T, Podgajny R, Bałanda M, Nakazawa Y, Miyazaki Y, Sorai M and Wasiutyński T 2004 *J. Magn. Magn. Mater.* **272–276** 1058
[5] Bałanda M, Korzeniak T, Pełka R, Podgajny R, Rams M, Sieklucka B and Wasiutyński T 2005 *Solid State Sci.* **7** 1113
[6] Bałanda M, Pełka R, Wasiutyński T, Nakazaka T, Miyazaki Y, Sorai M, Podgajny R, Korzeniak T and Sieklucka B, unpublished
[7] Luitjen E, Blöte H W J and Binder K 1997 *Phys. Rev. Lett.* **79** 561
[8] Le L P, Keren A, Luke G M, Wu W D, Uemura Y J, Tamura M, Ishikawa M and Kinoshita M 1993 *Chem. Phys. Lett.* **206** 405
[9] Bramwell S T and Holdsworth P C W 1993 *J. Phys.: Condens. Matter* **5** L53
[10] Campostrini M, Hasenbusch M, Pelissetto A, Rossi P and Vicari E 2001 *Phys. Rev.* B **63** 214503
[11] Hayano R S, Uemura Y J, Imazoto J, Nishida N, Yamazaki T and Kubo R 1979 *Phys. Rev.* B **20** 850
[12] Blundell S J, Pratt F L, Lancaster T, Marshall I M, Steer C A, Heath S L, Létard J-F, Sugano T, Mihailovic D and Omercu A 2003 *Polyhedron* **22** 1973–80
[13] Pratt F L 2007 *J. Phys.: Condens. Matter* **19** 456207
[14] Wildes A R, Rønnow H M, Roessli B, Harris M J and Godfrey K W 2007 *J. Magn. Magn. Mater.* **310** 1221
[15] Pratt F L, Baker P J, Blundell S J, Lancaster T, Green M A and Kurmoo M 2007 *Phys. Rev. Lett.* **99** 017202
[16] Pełka R, Bałanda M, Wasiutyński T, Nakazawa Y, Sorai M, Podgajny R and Sieklucka B 2004 *Czech. J. Phys.* **54** D595
[17] Berezinski B L 1971 *Sov. Phys.—JETP* **42** 493
Kosterlitz J M and Thouless D J 1994 *J. Phys.: Condens. Matter* **6** 1181
Kosterlitz J M 1995 *J. Phys.: Condens. Matter* **7** 1046
[18] Blundell S J, Lancaster T, Brooks M L, Pratt F L, Taliaferro M L and Miller J S 2006 *Physica* B **374/375** 114